Characterization of Low-Temperature Ultrananocrystalline™ Diamond RF MEMS Resonators

Sergio P. Pacheco [1], Peter Zurcher [1], Steven R. Young [2], Don Weston [2],
William J. Dauksher [2], Orlando Auciello [3], John A. Carlisle [3], Neil Kane [4], and James P. Birrell [4]

[1] Freescale Semiconductor, Inc. - Technology Solutions Organization, Tempe, AZ, 85284 USA
[2] Motorola, Inc. - Motorola Labs, Tempe, AZ, 85284 USA
[3] Argonne National Laboratory, Chicago, IL, 60439 USA
[4] Advanced Diamond Technologies, Inc., Champaign, IL, 61820 USA

Tel:(480) 413-3737, Fax:(480) 413-7918, email: Sergio.Pacheco@freescale.com

Abstract—
For the first time working MEMS resonators have been produced using low-temperature deposited (550°C) Ultrananocrystalline™ Diamond (UNCD™) films. Using a lumped-element model to fit experimental data, UNCD materials properties such as a Young's modulus of 710 GPa and an acoustic velocity of 14,243 m/s have been deduced. This is the highest acoustic velocity measured to date for a diamond MEMS structural layer deposited at low temperatures. A 10 MHz resonator shows a DC-tunability of the resonance frequency of 15% between 15 and 25 V and the breakdown voltage behavior shows electrostatic breakdown rather than electro-mechanical pull-down for higher frequency devices. Good resonant frequency reproducibility is observed when cycling the resonators over bias voltages from 15 to 25 V and over RF power levels of -10 to 10 dBm.

Keywords— MEMS resonator, resonant frequency, diamond, UNCD, acoustic velocity

I. INTRODUCTION

MEMS resonator technology has seen dramatic performance increases in the last few years. Devices such as radial and wine-glass resonators [1] have reached GHz frequencies while limiting increases in motional resistance. The fundamental limitation of this approach is the acoustic velocity of traditional MEMS structural materials, such as poly-Si. Hence, another strategy to increase performance is through the use of high acoustic velocity structural materials such as silicon carbide [2] and CVD polydiamond [3]. However, these films require high deposition temperatures ($\geq 800°C$) which makes them not suitable for integrated circuit back-end integration where temperatures $\leq 400°C$ are required.

We believe that UNCD has the potential of forming high acoustic velocity films at $400°C$ deposition temperature. This paper reports on a first step toward achieving such low temperature films through producing micromechanical resonators using $550°C$ UNCD films.

II. ULTRANANOCRYSTALLINE DIAMOND (UNCD)

UNCD thin films are deposited using microwave plasma chemical vapor deposition with argon-rich plasma chemistries and exhibit a microstructure with 2-5 nm equiaxed grains, atomically abrupt ($\sim$ 0.2-0.5 nm) grain boundaries, and smooth surfaces (RMS roughness $\sim$ 7-40 nm). A membrane deflection technique, applying a nanoin-denter on a MEMS scale UNCD membrane, was used to measure hardness as high as 98 GPa and Young's modulus as high as 980 GPa [4], both values close to those of single crystal diamond. In addition, the coefficient of fric-tion in air of as-deposited UNCD films is as low as 0.02 (similar to that of single crystal diamond), i.e., much lower than that of as-deposited microcrystalline diamond films ($\sim$ 0.5) [4][5].

III. RF MEMS RESONATOR DESIGN AND FABRICATION

As a first demonstration of UNCD-based resonators, sim-ple fixed-fixed beam devices were fabricated. The funda-mental mode resonant frequency for such devices can be written as [6]:

$$f_r = \frac{1}{2\pi}\sqrt{\frac{K_r}{m_r}} = \frac{1}{2\pi}\sqrt{\frac{K_m - K_e}{m_r}} \qquad (1)$$

$$K_m = 16EW_r\left(\frac{h}{L_r}\right)^3$$

$$K_e = \frac{\epsilon_0 W_r W_{el} V_d^2}{d^3}$$

where K_r is the overall effective beam stiffness, K_m is the effective beam stiffness without any bias voltage present, K_e is the "spring softening" term related to the restorative force acting on the beam due to the application of the bias voltage, m_r is the effective mass of the beam, E is the Young's modulus, L_r is the beam length, W_r is the beam width, h is the beam thickness, W_{el} is the electrode width, V_d is the drive or bias voltage, and ϵ_0 is the permittivity of air. Note that in the special limiting case of applied bias $V_d = 0$, equation 1 is equivalent to the natural fundamental mode of the beam:

$$f_r = f_0 = 1.03\sqrt{\frac{E}{\rho}}\frac{h}{L_r^2} \qquad (2)$$

where ρ is the beam material density.

Our MEMS resonator fabrication process is based on a surface micromachining technique very similar to the one used to fabricate laminate resonators described in previous work [7]. First, a 1.0 μm thick silicon nitride (SiN) iso-lation layer is deposited followed by a chromium/tungsten (Cr/W) thin film to form the electrode, anchor and metal conductors. Silicon dioxide (TEOS) is deposited over the metallization at the thickness required to define the criti-cal air-gap height ($\sim$ 120 nm) between the resonator beam and the drive electrode. Vias are formed over the conduc-tors to define the beam anchors. The beam consists of a sputtered layer of thin tungsten (50 nm) and a 1 μm thick

chemical vapor deposited UNCD layer at 550°C. The resonator beam is patterned using a multi-step dry plasma etch process. Finally, a wet HF-based release etch is used to remove the oxide sacrificial layer. Figure 1 shows a simplified schematic view of a processed resonator.
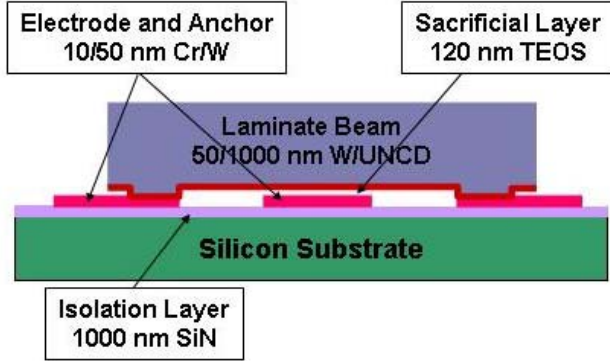

Fig. 1. Schematic cross-section of a MEMS fixed-fixed resonator device with typical process thickness of individual layers indicated.

IV. MEASURED DC AND RF PROPERTIES

A. DC Measurements

DC characterization is performed using a semiconductor parameter analyzer for beam breakdown, V_{bd}, (electrostatic breakdown or electro-mechanical pull-down) measurements. The pull-down voltage of resonator beams can be calculated as [8]:

$$V_{pd} = \sqrt{\frac{8}{27} \frac{K_d d^3}{\epsilon_0 W_r W_{el}}} \quad (3)$$

$$K_d = 32 E W_r \left(\frac{h}{L_r}\right)^3 \frac{1}{2 - \left[2 - \left(\frac{W_{el}}{L_r}\right)\right] \left(\frac{W_{el}}{L_r}\right)^2} \quad (4)$$

where K_d is the effective beam stiffness taking into account the distribution of the electrostatic force over the width of the biasing electrode. Fig. 2 shows a comparison between calculated pull-down voltage and measured resonator breakdown voltages for various designs ranging from 2 to 50 MHz. With a gap of 120 nm the average electric field applied during pull-down tests for designs below 20 MHz are below the danger zone of approximately 200 V/μm for electrostatic breakdown in sub-micron vacuum gaps [9]. In contrast, both 20 and 50 MHz designs indicate breakdowns of around 30 V on average; suggesting electrostatic failure, not mechanical pulldown. Such breakdown behavior is strongly affected by the geometry (corners) and surfaces (roughness, work function) of the gap structures; hence small process variations and defects could lead to catastrophic failure of higher frequency devices.

B. RF Measurements

RF characterization is performed in a custom-built vacuum chamber with a base pressure of 20 mTorr. Both input and output RF signals are provided and measured by a vector network analyzer. The RF transmission spectrum (S21) is used to determine resonance frequency and
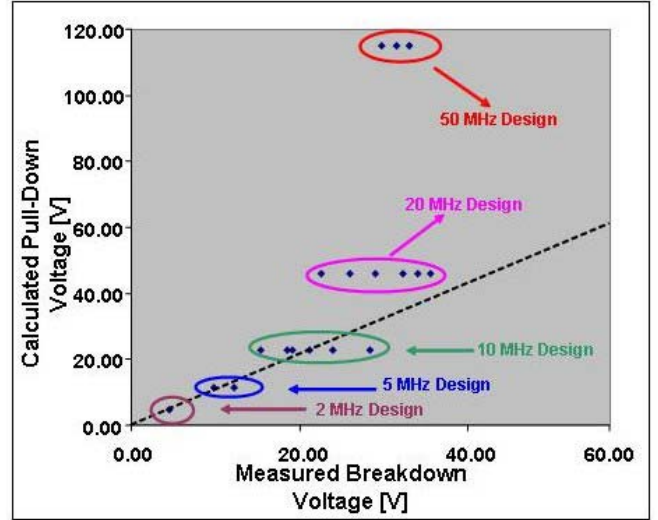

Fig. 2. Comparison between calculated pull-down voltage and measured breakdown voltages for various resonator designs ranging from 2 to 50 MHz.

Q of the device. Furthermore, a lumped element electrical model based on a force-voltage analogy is used to simulate the mechanical resonator as a series L-C-R resonant circuit. The model also includes the resonator static capacitance C_0, and parasitic elements such as bond-pad capacitance C_p and substrate resistance R_p [7]. Fig. 3 is a schematic of the lumped element model for the MEMS resonator. The formulas indicate the relationship between mechanical and electrical elements of the model. The electromechanical coupling coefficient η relates the two quantities and is extremely sensitive to variations in the gap d. The model is
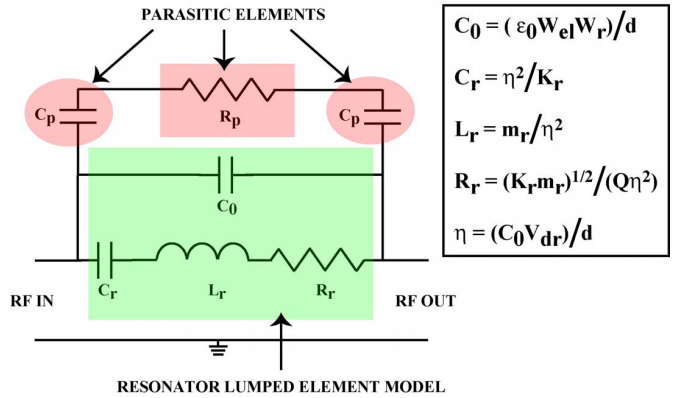

Fig. 3. Schematic of lumped element model for the MEMS resonator.

implemented using a circuit simulator and has been used to successfully predict the RF response of the resonating devices. Fig. 4 shows a comparison of the measured and modelled RF spectrum of a device with resonant frequency at 8.72 MHz. It is important to note here that the Q value of the resonator is relatively low. We believe this is due to a non-optimal release etch process. At the present time, the devices are released via a wet etch (see section III) and then coated with a thick resist protection layer for singulation. After singulation, the resist is removed and the individual die mounted and tested. This release/dicing
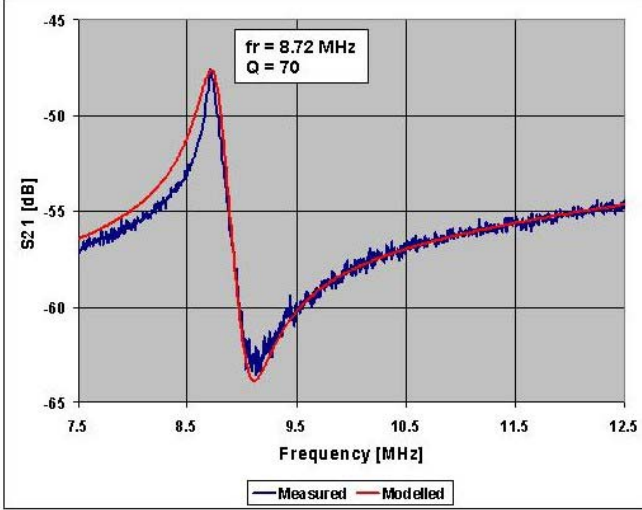
Fig. 4. Measured and modelled resonant frequency and Q of a UNCD device with a resonant frequency at 8.72 MHz. Measurements were performed with a drive voltage of 25 V and RF power level of -10 dBm. Model parameters are: E=710 GPa, ρ=3500 kg/m^3, h=0.87 μm, and d=130 nm.

process could potentially result in not completely "clean" structures. A similar issue was encountered when processing previous TaN/SiON laminate beams and was resolved by moving to a dry etch release that occurred after singulation. In that case, fixed-fixed laminate beam resonators saw a marked increase in Q [7]. Different options are being evaluated presently, from dry etching of the oxide sacrificial layer to the use of critical-point drying, in order to mitigate the issues with the current release etch process.

Fig. 5 shows: (a) the RF response of the resonator with varying bias voltages and RF power set at -10 dBm, and (b) the comparison between measured and modelled resonant frequencies for that same device. The total change in resonant frequency over the 15 to 25 V bias voltage range is 15.7%. Assuming a theoretical density of 3500 kg/m^3, the derived UNCD Young's modulus from the model for both devices in Figs. 4 and 5 is 710 GPa which corresponds to an acoustic velocity of 14,243 m/s. This is the highest acoustic velocity to date for a diamond film deposited at temperatures below 600°C.

Equivalently, measurements were performed on the same device with varying RF power levels from -10 to 0 dBm with the bias voltage set at 20 V. The total resonant frequency variation over the range of RF power levels was 2.37%. This can be explained by the fact that the resonator "sees" an increased DC bias by the average voltage of the rectified RF signal as given by [10]:

$$V_{avg} = \frac{1}{T} \int_0^{T/2} V_p sin(wt)dt = \frac{V_p}{\pi} \qquad (5)$$

where $T = 2\pi/\omega$ is the period of the RF signal. The RF power in terms of peak voltage, V_p, given by:

$$P = \frac{V_p^2}{2Z} \qquad (6)$$

where Z is the characteristic impedance of the electrode and for the frequencies of interest (10-50 MHz) is approximately 125 Ω. Using (5), and solving for V$_{avg}$, the following
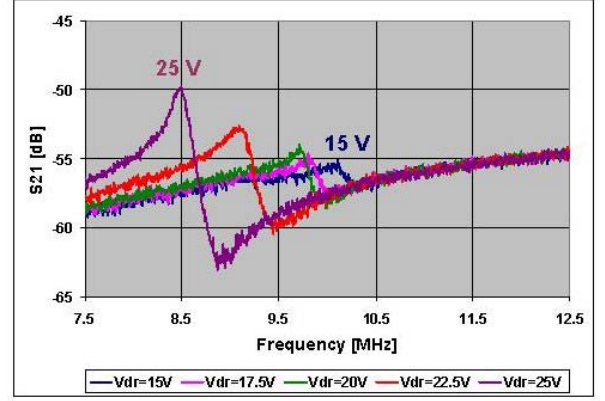
(a) UNCD Resonator RF Response

(b) Measured vs. Modelled Resonant Frequency

Fig. 5. Plots showing (a) RF response of UNCD resonator with varying bias voltages and RF power set at -10 dBm, and (b) comparison of measured and modelled resonant frequencies for the resonator in (a). Model parameters are: E=710 GPa, ρ=3500 kg/m^3, h=0.87 μm, and d=127 nm.

equation can therefore be used to determine the amount of average voltage derived from the RF power:

$$V_{avg} = \frac{\sqrt{2ZP}}{\pi} \qquad (7)$$

From equation 7, the calculated average voltages for -10 and 0 dBm are 0.05 and 0.16 V, respectively. These voltages are small compared to the bias voltages and contribute to a small shift in frequency. However, RF power levels become critical for low bias devices, where the above average voltages are very close or above the pull-down/breakdown voltage. For example, assuming that the drive voltage V_{dr} needs to be at least 50% of the pull-down voltage for adequate electromechanical coupling and that the total voltage including the average voltage derived from RF power ($V_{tot} = V_{dr} + V_{avg}$) to be less than about 85% of the pull-down for reliability reasons, then the maximum allowable RF power for a 2 MHz device is 19 dBm or 77 mW. This clearly indicates a limitation in the applicability of such resonators, especially if they are intended to work as filters

(diplexers/duplexers) in the transmit chain. This limitation will need to be addressed in more detail in the future.

We have performed several reproducibility measurements on two different resonators by cycling the devices several times through varying bias voltage and RF power level conditions. The bias cycling measurements consisted of ramping the drive voltage from 15 to 25 V (in 2.5 V steps) at a power level of -10 dBm for a total of 5 cycles on a 10 MHz device. The RF power cycling consisted of increasing the power level from -10 to 10 dBm (in 5 dBm steps) at a bias voltage of 20 V for a total of 3 cycles on a 30 MHz device. Table I summarizes the maximum resonant frequency variation at each bias voltage and RF power setting (not to be confused with the change in resonant frequency as a function of applied bias).

TABLE I

MAXIMUM VARIATION IN RESONANT FREQUENCY AT DISCRETE BIAS VOLTAGES AND RF POWER LEVELS DURING CYCLING MEASUREMENTS

Bias Voltage [V] (@ -10 dBm)	Maximum Frequency Variation over Cycles 1-5 [%]	RF Power [dBm] (@ 20 V)	Maximum Frequency Variation over Cycles 1-3 [%]
15.0	0.14	-10	0.14
17.5	0.47	-5	0.13
20.0	0.64	0	0.10
22.5	1.00	5	0.09
25.0	0.62	10	0.10
Average Variation [%]	0.57	Average Variation [%]	0.11

In both cases, the UNCD MEMS resonator shows acceptable reproducibility; however, additional measurements must be performed to determine the long-term stability of the devices.

V. CONCLUSIONS

In this work we have demonstrated the first RF MEMS resonators built with a high acoustic velocity UNCD films that were deposited at low temperatures. A lumped-element model has been developed that provides very good agreement with experimental results on frequency tuning and pull-down voltage of MHz resonators. Furthermore, the low-temperature budget for the fabrication process as well as the use of CMOS-compatible films points toward future integration opportunities.

ACKNOWLEDGEMENTS

REFERENCES

[1] J. Wang et. al., "1.156-GHz Self-Aligned Vibrating Micromechanical Disk Resonator," *IEEE Transactions on Ultrasonics, Ferroelectrics and Frequency Control*, vol. 51, no. 12, pp. 1607–1628, December 2004.

[2] S. Roy et. al., "Fabrication and Characterization of Polycrystalline SiC Resonators," *IEEE Transactions on Electron Devices*, vol. 49, no. 12, pp. 2323–2332, December 2002.

[3] J. Wang et. al., "1.51-GHz Nanocrystalline Diamond Micromechanical Disk Resonator With Material-Mismatched Isolating Support," in *Proceedings of the 17th IEEE International Conference on Micro Electro Mechanical Systems*, 2004, pp. 641–644.

[4] O. Auciello et. al., "Materials Science and Fabrication Processes for a New MEMS Technology Based on Ultrananocrystalline Diamond Thin Films," *Journal of Physics: Condensed Matter*, pp. R539–R552, 2004.

[5] A. Sumant et. al., "Toward the Ultimate Tribological Interface: Single Asperity Properties and Surface Chemical Optimization of Ultrananocrystalline Diamond," *Advanced Materials (in press)*, 2004.

[6] K. Wang et. al., "VHF Free-Free Beam High-Q Micromechanical Resonators," in *Proceedings of the IEEE MEMS Conference*, 1999, pp. 453–458.

[7] S. Pacheco et. al., "RF MEMS Resonator for CMOS Back-End-Of-Line Integration," in *Proceedings of the 5th Topical Meeting on Silicon Monolithic Integrated Circuits in RF Systems*, 2004, pp. 203–206.

[8] N. S. Barker, *Distributed MEMS Transmission Lines*, Ph.D. thesis, University of Michigan, 1999.

[9] T. Ono et. al., "Micro-discharge and Electric Breakdown in a Micro-gap," *Journal of Micromechanics and Microengineering*, vol. 10, no. 3, pp. 445–451, 2000.

[10] S. P. Pacheco, *Design and Fabrication of Low Actuation Voltage K-Band MEMS Switches for RF Applications*, Ph.D. thesis, University of Michigan, 2004.